nounced after protonation, making the molecular edifice stable and rigid, whereas the free catenand is highly flexible. Interestingly, the same phenomenon holds for $1{\cdot}H_2^{2+}$, the electrostatic repulsion between the two bound protons being compensated by a stronger acceptor–donor interaction. It might even be predicted that with highly positively charged species as complexed moieties, a strong additional stabilization (energy and rigidity) arising from intramolecular charge transfer should be observed.

Conclusion

The catenand **1** undergoes a complete rearrangement by protonation, $1{\cdot}H^+$ and $1{\cdot}H_2^{2+}$ being proton catenates whose dpp fragments are entwined around the proton(s). The special shape of $1{\cdot}H^+$, as studied by X-ray crystallography and ^1H NMR, is highly stabilized with respect to the acyclic analogue **2**. This topological effect is very effective both for the mono- and the diprotonated species. An illustration of the catenand effect is found in the unusually high basicity observed for phenanthroline sites. Although the catenand **1** is a flexible molecular system, for which each ring is able to glide freely within the other, the molecular edifice obtained after protonation is rigid and surprisingly stable. An unexpected but strong contribution to the stabilization originates in a charge-transfer interaction. This interaction is remote from the protonation site, but its strength is much dependent on the protonation degree. Such an example, for which simple protonation processes entirely govern the geometry of the molecular system as well as intramolecular interactions, might be generalized to other cases more relevant to biological problems.

Registry No. $1{\cdot}HClO_4$, 103733-28-4.

Structures of Alumina-Supported Osmium Clusters ($HOs_3(CO)_{10}\{OAl\}$) and Complexes ($Os^{II}(CO)_{n=2or3}\{OAl\}_3$) Determined by Extended X-ray Absorption Fine Structure Spectroscopy

F. B. M. Duivenvoorden,† D. C. Koningsberger,*† Y. S. Uh,‡ and B. C. Gates‡

Contribution from the Laboratory for Inorganic Chemistry and Catalysis, Department of Chemical Technology, Eindhoven University of Technology, 5600 MB Eindhoven, The Netherlands, and Center for Catalytic Science and Technology, Department of Chemical Engineering, University of Delaware, Newark, Delaware 19716. *Received November 19, 1985*

Abstract: EXAFS measurements have been carried out with $Os_3(CO)_{12}$, the supported cluster $HOs_3(CO)_{10}\{OAl\}$ prepared by reaction of $Os_3(CO)_{12}$ with γ-Al_2O_3, and the supported sample after decomposition in He at 150 °C. The data were analyzed by applying phase- and/or amplitude-corrected Fourier transforms together with the difference file technique for reliable separation of the various contributions in the composite EXAFS spectrum. Phases and backscattering amplitudes were obtained from reference compounds; the reference for the Os—C≡O moiety was derived from $Os_3(CO)_{12}$. The results are consistent with the surface structure $HOs_3(CO)_{10}\{OAl\}$, postulated previously. The Os—Os and Os—C≡O coordination distances in the cluster do not change upon reaction of $Os_3(CO)_{12}$ with the support; two osmium atoms of the cluster are coordinated to a bridging oxygen anion at an average Os—O distance of 2.16 Å. After decomposition of the supported cluster, the Os—Os oscillations disappeared from the spectrum. The average Os—C≡O coordination number for the osmium ion (valence state presumably +2) was found to be 2.8. The osmium ion was surrounded by three support oxygen neighbors at an average distance of 2.17 Å.

Introduction

Supported metal catalysts used in many large-scale processes consist of small (~10–1000 Å) aggregates or crystallites of metal dispersed on high-surface-area metal–oxide supports. Since the metal aggregates are nonuniform in size, shape, and catalytic properties, the best attainable relations between structure and catalytic performance have been based on the average structural properties which are inferred—sometimes tenuously—from indirect structure probes. Only for very small aggregates of structurally simple supported metals are structures well defined; X-ray absorption spectroscopy, combined with other physical methods, has been decisive in the structure determinations.[1-3]

Alternatively, supported organometallic species analogous to molecular structures are attractive as model supported metal catalysts offering several advantages with respect to fundamental understanding of structure and performance: (1) the structure can, in prospect, be determined with precision, on the basis of comparisons of sample spectra and those of fully characterized molecular analogues; (2) the nature of the bonding between the organometallic species and the support can be determined with precision on the basis of comparisons of specta of surface species with those of analogous molecular structures incorporating ligands similar to those of the functional groups terminating the support surface. Therefore, the often ill-defined issues related to the structure of supported metal catalysts and metal–support interactions can be placed on a firm fundamental foundation.

The supported "molecular" organometallics that have been characterized most thoroughly are triosmium clusters anchored to silica and to alumina.[4-9] The structure has been inferred to

* To whom correspondence should be addressed.
† Eindhoven University of Technology.
‡ University of Delaware.

(1) Van Zon, J. B. A. D.; Koningsberger, D. C.; Van 't Blik, H. F. J.; Sayers, D. E. *J. Chem. Phys.* **1985**, *82*, 5742.
(2) Via, G. H.; Sinfelt, J. H.; Lytle, F. W. *J. Chem. Phys.* **1979**, *71*, 690.
(3) Sinfelt, J. H.; Via, G. H.; Lytle, F. W.; Greegor, R. B. *J. Chem. Phys.* **1981**, *75*, 5527.
(4) Psaro, R.; Ugo, R. *Metal Clusters in Catalysis*; Gates, B. C., Guczi, L., Knözinger, H., Eds.; Elsevier: Amsterdam, in press.
(5) Psaro, R.; Ugo, R.; Zanderighi, G. M.; Besson, B.; Smith, A. K.; Basset, J. M. *J. Organomet. Chem.* **1981**, *213*, 215.
(6) Deeba, M.; Gates, B. C. *J. Catal.* **1981**, *67*, 303.
(7) Knözinger, H.; Zhao, Y. *J. Catal.* **1981**, *71*, 337.
(8) Deeba, M.; Streusand, B. J.; Schrader, G. L.; Gates, B. C. *J. Catal.* **1981**, *69*, 218.

0002-7863/86/1508-6254$01.50/0

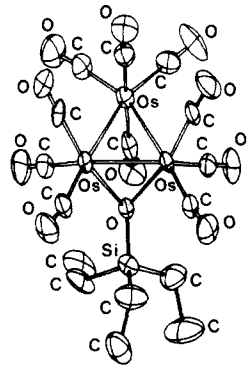

Figure 1. Structure of $HOs_3(CO)_{10}OSiEt_3$,[11] with Os–Os distances 2.816, 2.820, and (oxygen bridged) 2.777 Å.

be the following from (1) the stoichiometry of the synthesis from $Os_3(CO)_{12}$ and surface OH groups (splitting off two CO ligands),[5] (2) infrared spectra in the carbonyl region,[5-7] (3) Raman spectra indicating Os–Os bonds,[8] and (4) observations by high-resolution electron microscopy, indicating surface structures with the size of the clusters and no larger metal structures.[9,10] All the spec-

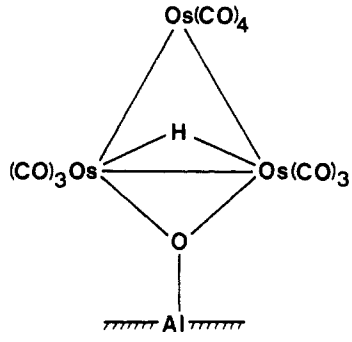

troscopic results were interpreted by comparison with spectra of analogous compounds with known crystal structures, such as $HOs_3(CO)_{10}(OH)$. Recently, the crystal structure of an excellent analogue of the silica-supported cluster, $HOs_3(CO)_{10}OSiEt_3$, has been reported (Figure 1).[11]

This surface structure should perhaps be regarded as well established, but a complete characterization requires a confirmation by X-ray absorption spectroscopy, which can in prospect determine the average interatomic distances and the metal oxidation states in the surface organometallic structures. There are two communications[12,13] reporting EXAFS (Extended X-ray Absorption Fine Structure) spectra of oxide-supported triosmium clusters. The results do not provide clear and convincing confirmation of the structure suggested above, although they are consistent with this and similar structures.

Besson et al.[5,12] reported EXAFS results confirming the presence of triosmium clusters on silica and showing the absence of osmium metal particles. The average Os–Os distance in the supported cluster was inferred to be 2.68 Å, whereas the distance in the presumed molecular analogue $HOs_3(CO)_{10}OSiEt_3$ is 2.777 Å for the oxygen-bridged osmiums, the other osmium–osmium distances being 2.820 and 2.816 Å.[11]

Cook et al.[13] used EXAFS to characterize triosmium clusters supported on γ-alumina. They fitted their data in k space using theoretically calculated values of the phase shift and backscattering amplitude and a theoretical calculation of the multiple scattering between carbon and oxygen. With these theoretically calculated values, they inferred an average Os–Os distance of 2.84 Å. They suggested that the surface structure analogous to that shown in Figure 1 might be accompanied by a surface structure incorporating two bridging oxygen ions of the surface; this latter structure has not been suggested by other authors.

The reactivity and catalytic activity of the oxide-bound cluster $HOs_3(CO)_{10}\{OAl\}$ have been investigated in some detail.[5-9,14-16] On the basis of the stoichiometry of the reaction,[5] infrared spectra,[5-7] and Raman spectra,[8] it has been inferred that heating of the supported cluster to about 120 °C (the value is support-dependent) in vacuum or He leads to breaking of the Os–Os bonds, oxidation of the osmium to the divalent state, and evolution of CO and H_2. Surface OH groups are the oxidizing agent. The resulting structure has been postulated[5-9] to be $Os^{II}(CO)_n$, where $n = 2$ or 3. Infrared spectroscopy has been used to establish details of the structure of this mononuclear surface complex and to follow the reversible carbonylation–decarbonylation process.[7] Electron micrographs of these broken-up clusters on γ-alumina suggested the presence of three-atom ensembles of Os; the Os ions were inferred to have remained on the surface very nearly where the clusters were originally bonded.[9,10] The reconstitution of a fraction of the clusters induced by CO was taken as evidence confirming the presence of these ensembles.[14]

To provide a more nearly definitive structural characterization of these surface species, we have performed EXAFS experiments with $Os_3(CO)_{12}$, the alumina-supported triosmium cluster, and the broken-up cluster on alumina. We report here the results with full details of the data analysis procedure. Experimentally determined phases and backscattering amplitudes were used for the analysis of the EXAFS data characterizing the alumina-supported cluster and the broken-up cluster. $Os_3(CO)_{12}$ was used as an experimental reference for the Os—C≡O coordination. To determine reliably the contributions to the EXAFS spectrum arising from the various groups coordinated to osmium, the difference file technique was applied[1] together with phase- and/or amplitude-corrected Fourier transforms.

The results confirm the earlier structural conclusions and cast doubt on the EXAFS results published for the alumina-supported osmium cluster. Detailed information has also been obtained that characterizes the structure of the broken-up cluster on alumina, in particular the coordination of osmium with support oxygen ions.

Experimental Section

Materials and Catalyst Preparation. $Os_3(CO)_{12}$ was obtained from Strem and used without further purification. *n*-Octane (Fisher analyzed) was freshly dried and redistilled in the presence of metallic sodium under N_2. Dichloromethane (Fisher analyzed) was freshly dried and redistilled in the presence of phosphorus pentoxide under nitrogen.

The γ-alumina used as a support was grade D supplied by Ketjen; the BET surface area was about 250 m^2/g. The alumina was treated for 5 h in flowing oxygen at 400 °C, purged with N_2 for 2 h at 400 °C, cooled to room temperaure under vacuum, and then transferred under N_2 to a drybox. For the preparation of the catalyst, 4 g of Al_2O_3, 65.3 mg of $Os_3(CO)_{12}$, and 200 mL of *n*-octane were added to a 500-mL flask in the absence of air. The mixture was stirred and refluxed or 90 min. Upon refluxing, the deep yellow solution became colorless and the solid particles yellow. These observations suggest that most of the cluster had been adsorbed on the alumina. The slurry was transferred under nitrogen to a Soxhlet apparatus, where the solid was extracted with dichloromethane for 10 h to remove physisorbed cluster. The extract solutions were pale yellow. The resulting solid, containing about 1 wt % Os, was dried under vacuum for 10 h and then stored under N_2 in a drybox. A fraction of the sample was held for 5 h at 150 °C in a calcining tube for thermal decomposition of the surface-bound cluster; this sample was also handled under N_2.

Infrared Spectroscopy. Infrared spectra of self-supporting wafers were measured with a Nicolet 7199 Fourier transform spectrophotometer. The details of the cell design are reported by Barth et al.[14] The samples were self-supporting wafers. The spectral resolution was 4 cm^{-1}. The spectrum

(9) Knözinger, H.; Zhao, Y.; Tesche, B.; Barth, R.; Epstein, R.; Gates, B. C.; Scott, J. P. *Faraday Discuss.* **1981**, *72*, 53.
(10) Schwank, J.; Allard, L. F.; Deeba, M.; Gates, B. C. *J. Catal.* **1983**, *84*, 27.
(11) D'Ornelas, L.; Choplin, A.; Basset, J. M.; Hsu, L.-Y.; Shore, S. *Nouv. J. Chim.* **1985**, *9*, 155.
(12) Besson, B.; Moraweck, B.; Smith, A. K.; Basset, J. M.; Psaro, R.; Fusi, A. *J. Chem. Soc., Chem. Commun.* **1980**, 569.
(13) Cook, S. L.; Evans, J.; Greaves, G. N. *J. Chem. Soc., Chem. Commun.* **1983**, 1287.
(14) Barth, R.; Gates, B. C.; Zhao, Y.; Knözinger, H.; Hulse, J. *J. Catal.* **1983**, *82*, 147.
(15) Li, X. J.; Gates, B. C. *J. Catal.* **1983**, *84*, 55.
(16) Li, X. J.; Onuferko, J. H.; Gates, B. C. *J. Catal.* **1984**, *85*, 176.

of the sample prepared from $Os_3(CO)_{12}$ and γ-Al_2O_3 compares very well with spectra of previous reports.[5,6] The spectrum of the decomposed cluster on alumina is similar to published spectra,[5-7] indicating the presence of mononuclear osmium complexes on the support.

EXAFS. The experiments were carried out at EXAFS station I-5 at the Stanford Synchrotron Radiation Laboratory (SSRL), with a ring energy of 3 GeV and ring currents between 40 and 80 mA. A Si(220) channel-cut monochromator with a d spacing of 1.92 Å was employed.

The powder was pressed into self-supporting wafers to give samples of good uniformity. The wafer thickness was chosen to give a total X-ray absorbance of about 1. An EXAFS sample cell allowed measurements at liquid-nitrogen temperatures and in situ treatments of the sample at elevated temperatures to decompose the supported cluster in a helium atmosphere. The data collection time for each run was about 25 min. Experiments were carried out with the alumina-supported cluster, the decomposed cluster, and a reference material consisting of a physical mixture of approximately 1 wt. % crystalline $Os_3(CO)_{12}$ with silica powder.

Data Analysis

Data Analysis Procedure. A general expression for the measured EXAFS $\chi(k)$ has been given by Stern et al.[17-19] (eq 1). The

$$\chi(k) = \sum_j A_j(k) \sin (2kR_j + \phi_j(k)) \quad (1)$$

EXAFS function is a superposition of contributions from different coordination shells; the index j refers to the jth coordination shell. R_j is the average coordination distance between the absorbing atom and the neighboring atoms in the jth coordination shell, $\varphi_j(k)$ is the phase shift which the photoelectron experiences during the scattering process, and $A_j(k)$ is the amplitude function, which is expressed as in eq 2. N_j is the average number of scatterer atoms

$$A_j(k) = \frac{N_j}{kR_j^2} S_0^2(k) F_j(k) e^{-2k^2\sigma_j^2} e^{-2(R_j-\Delta)/\lambda} \quad (2)$$

in the jth coordination shell. σ_j^2 is the mean square deviation about the average coordination distance R (caused by themal motion and/or static disorder). $F_j(k)$ is the backscattering amplitude characteristic of a particular type of neighboring atom. $S_0^2(k)$ is a correction for the relaxation of the absorbing atom and multielectron excitations.[20] λ is the mean free path of the photoelectron. Δ is a correction term ($\Delta \simeq R_1$) in the mean free path concept, which is used because $S_0^2(k)$ and $F_j(k)$ already account for most of the photoelectron losses in the first coordination shell. The expression is valid for the case of small disorder with a Gaussian pair distribution function.[21-24]

In order to separate the contributions from different shells, the EXAFS function $\chi(k)$ is Fourier transformed. The Fourier transform $\theta_n(r)$ is expressed as in eq 3. A k^n weighting (usually

$$\theta_n(r) = \frac{1}{2\pi^{1/2}} \int_{k_{min}}^{k_{max}} k^n \chi(k) e^{2ikr} dk \quad (3)$$

n = 1, 2, or 3) is used to equalize the envelope of $\chi(k)$ over the transformation range, with n depending on the amplitude variation and signal-to-noise ratio of the measured signal. The function $\theta_n(r)$ will contain peaks which are related to the actual coordination distances R_j, but these peaks are shifted toward lower r values due to the influence of the phase shift $\phi_j(k)$ in eq 1.[25] The exact values of R and N for a shell of scatterer atoms j can be found when the phase shift $\phi_j(k)$ and backscattering amplitude $F_j(k)$ for the absorber–scatterer pair are known; $\phi_j(k)$ and $F_j(k)$ can be calculated theoretically,[26] or can be extracted from EXAFS data for a reference compound with known structure.

To obtain the phase shift and backscattering amplitude experimentally, the EXAFS data of the reference compound are Fourier transformed according to eq 3. In the resulting spectrum in r space, the peak representing the atoms for which a reference is needed is back transformed to k space between suitable values of R_{min} and R_{max} (eq 4). This step requires a spectrum in r space

$$k^n\chi(k) = \frac{1}{2\pi^{1/2}} \int_{R_{min}}^{R_{max}} \theta_n(r) e^{-2ikr} dr \quad (4)$$

in which the peak of interest is well separated from all other peaks. When the chemical state of the absorber–scatterer pair under observation does not differ too much in the unknown and reference compound, then only N, R, and σ^2 will differ in eq 1 and 2.[17] N_{ref} and R_{ref} are known because the structure of the reference compound is known. Thus, using a reference compound we obtain N and R of an unknown shell directly and σ^2 of this unknown shell relative to that of the reference compound. We consider empirically determined phases and amplitudes to be more reliable than those determined theoretically.[26]

To analyze an EXAFS spectrum composed of different contributions giving a strong overlap of the corresponding peaks in r space after Fourier transformation, one normally uses the technique of fitting in k space. In such a fitting process, a multiple-shell formula such as eq 1 is fitted to the experimental EXAFS signal. A large number of adjustable parameters must be estimated in this process, and it is well possible that small differences in k space, not associated with the fitted coordination distances, may be compensated by incorrect parameter values. In order to check the reliability of the parameters obtained by fitting in k space, one has to compare the Fourier transform (the imaginary part as well as the magnitude) of the experimental results with the corresponding transform of the EXAFS function calculated with the parameter values found by fitting in k space. We have found that a reliable separation of the different contributions in an EXAFS spectrum can be obtained by applying the difference file technique[1,27] and using phase- and/or amplitude-corrected Fourier transforms.

A phase- and amplitude-corrected Fourier transform can be obtained when $\chi(k)$ in eq 3 is substituted by[1,28-30]

$$\chi(k)\frac{e^{-i\phi(k)}}{F_j(k)}$$

A Fourier transform, phase- and amplitude-corrected for an X–Y absorber–scatterer pair, yields the following features: (1) Peaks which have a positive imaginary part of the Fourier transform (peaking at the maximum of the magnitude of this Fourier transform) are due to neighbors of atom type Y. These peaks have their maxima at the correct X–Y distance. (2) Peaks which are not symmetrical are a superposition of more than one contribution. Thus, the use of corrected Fourier transforms can be a great help in the identification of different types of neighbors by application of different phase and/or amplitude corrections.

To analyze a composite EXAFS spectrum, we further use the difference file technique. In this technique, the parameters R, N, and $\Delta\sigma^2$ (relative to the reference compound) of the largest contribution in the spectrum are first estimated from a spectrum in r space (obtained by Fourier transformation, phase- and/or amplitude-corrected for the atom type which causes the largest contribution). When the estimated parameters are judged to be satisfactory, an EXAFS function calculated with these parameters is subtracted from the experimental EXAFS signal. In the re-

(17) Stern, E. A.; Bunker, B. A.; Heald, S. M. *Phys. Rev. B* **1980**, *21*, 5521.
(18) Stern, E. A. *Phys. Rev. B* **1974**, *10*, 3027.
(19) Lytle, F. W.; Sayers, D. E.; Stern, E. A. *Phys. Rev. B* **1975**, *11*, 4825.
(20) Cook, J. W., Jr.; Sayers, D. E. *J. Appl. Phys.* **1981**, *52*, 5024.
(21) Eisenberger, P.; Brown, G. S. *Solid State Commun.* **1979**, *29*, 481.
(22) Crozier, E. D.; Seary, A. J. *Can. J. Phys.* **1980**, *58*, 1388.
(23) Crozier, E. D.; Seary, A. J. *Can. J. Phys.* **1981**, *59*, 876.
(24) Bouldin, C.; Stern, E. A. *Phys. Rev. B* **1982**, *25*, 3462.
(25) Stern, E. A.; Sayers, D. E.; Lytle, F. W. *Phys. Rev. B* **1975**, *11*, 4836.
(26) Teo, B. K.; Lee, P. A. *J. Am. Chem. Soc.* **1979**, *101*, 2815.
(27) Van 't Blik, H. F. J.; Van Zon, J. B. A. D.; Huizinga, T.; Vis, J. C.; Koningsberger, D. C.; Prins, R. *J. Am. Chem. Soc.* **1985**, *107*, 3139.
(28) Lee, P. A.; Beni, G. *Phys. Rev. B* **1977**, *15*, 2862.
(29) Lytle, F. W.; Greegor, R. B.; Marques, E. C.; Sandstrom, D. R.; Via, G. H.; Sinfelt, J. H. *J. Catal.* **1985**, *95*, 546.
(30) Pendry, J. B. *EXAFS for Inorganic Systems (Proceedings of the Daresbury Study Weekend 28–29 March 1981)*; Garner, C. D., Hasnain, S. S., Eds.; Science and Engineering Research Council, Daresbury Laboratory: Daresbury, England, 1981; p 5.

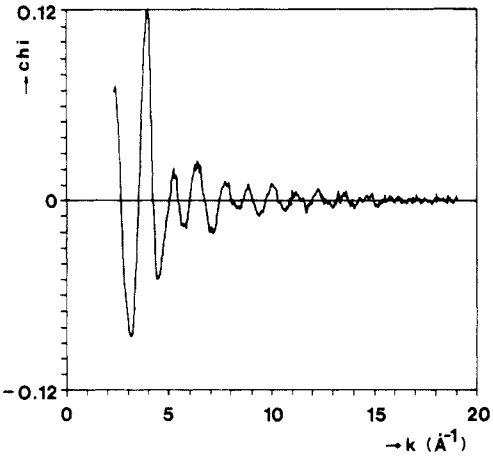

Figure 2. Raw EXAFS of a physical mixture of $Os_3(CO)_{12}$ and SiO_2.

maining signal, again the largest contribution is *estimated*. It may be necessary, especially for superposed contributions, to alter slightly the parameters of previously calculated shells. In the end this iterative process results in a set of best parameters. During the iteration, the agreement in k space is regularly checked. The calculated EXAFS signal, composed of the different contributions, should agree as well as possible with the experimental result in k space *and* in r space.

It is our experience that theoretical phase shifts and backscattering amplitudes are not reliable enough (especially at low values of k) for the data analysis procedure described above. Moreoever, in the case of $Os_3(CO)_{12}$ and related compounds, the use of reference compounds yields an extra advantage. In $Os_3(CO)_{12}$ the Os–C–O angle is 169°.[31] Thus, multiple scattering is expected, and indeed observed, for the Os–O shell.[32-34] Since multiple scattering contributions are difficult to calculate quantitatively, use of a reference compound is preferable.

In this work we used as reference compounds $Os_3(CO)_{12}$, Pt foil, and $Na_2Pt(OH)_6$. From the $Os_3(CO)_{12}$ data, a reference was extracted for the Os—C≡O moiety, as outlined below. We used Pt foil data[35] to estimate the Os–Os contributions and $Na_2Pt(OH)_6$ data[36] to estimate the Os–$O_{support}$ contributions. These references were used because Os metal and Os oxide data measured under the same experimental conditions at the same EXAFS station were not available. We justify the choice of our references in the Discussion.

Results

Os–CO Reference. A physical mixture of $Os_3(CO)_{12}$ and SiO_2 was characterized to provide a reference for the Os–CO shell. The EXAFS spectrum (Figure 2) is a superposition of an Os–Os and an Os–CO contribution. Separation of these two contributions is not straightforward because the Os–Os and Os–O peaks in r space (after Fourier transformation) are superimposed. Even a k^3 weighted transform, which should separate the Os–Os and Os–O peaks as well as possible, is not sufficient (Figure 3a).

The best way to separate the contributions was found to be an estimation of the Os–Os contribution in k space. Since C and O cause negligible backscattering at values of k greater than ~10–11 Å^{-1},[26] the EXAFS spectrum for $k > 11$ Å^{-1} is almost entirely due to the Os–Os shell. The crystal structure provides the data for the Os–Os coordination:[31] $N_{Os-Os} = 2$, $R_{Os-Os} = 2.88$ Å. With these parameters, a best estimate for the Os–Os shell was calculated. A Debye–Waller factor ($\Delta\sigma^2$) of −0.001 Å^2 (relative to Pt foil) was used, which gave the best agreement with the EXAFS data for $k > 11$ Å^{-1} (Figure 4).

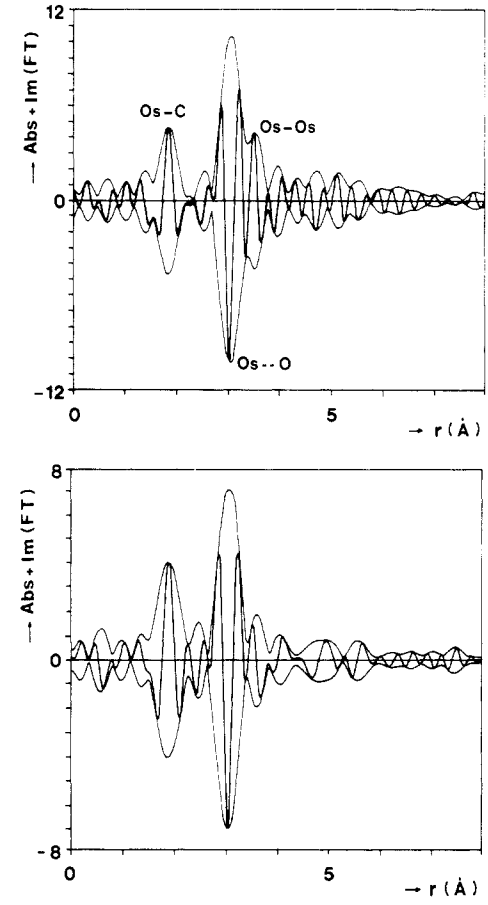

Figure 3. k^3 Fourier transform (Os–O phase corrected) of (a, top) the $Os_3(CO)_{12}$ data (Δk = 3.72–12.55 Å^{-1}) and (b, bottom) the $Os_3(CO)_{12}$ data minus calculated Os–Os shell (Δk = 3.75–11.89 Å^{-1}).

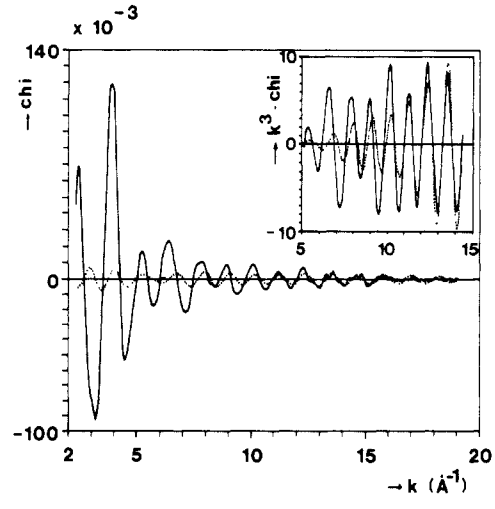

Figure 4. EXAFS of $Os_3(CO)_{12}$ (solid line) and calculated Os–Os shell (N = 2, R = 2.88 Å, $\Delta\sigma^2$ = −0.001 Å^2 relative to Pt foil) (dotted line).

After subtraction of the calculated Os–Os contribution from the experimental results, a Fourier transform was again applied, with a k^3 weighting used to separate the Os–C and Os–O peaks in r space as well as possible. By use of an Os–O phase correction, a peak pattern should be obtained in r space with two symmetrical imaginary parts, one with a positive peak (the Os–C shell) and one with a negative peak (the Os–O shell). The negative imaginary part of the Os–O peak is due to the multiple scattering contribution (see Discussion). To get perfectly symmetrical peaks in the Fourier transform (k^3, Δk = 3.75–11.89 Å^{-1}, Os–O phase corrected) of our difference spectrum, small V_0 corrections were

(31) Corey, E. R.; Dahl, L. F. *Inorg. Chem.* **1962**, *1*, 521.
(32) Lee, P. A.; Pendry, J. B. *Phys. Rev. B* **1975**, *11*, 2795.
(33) Teo, B. K. *J. Am. Chem. Soc.* **1981**, *103*, 3990.
(34) Cramer, S. P.; Hodgson, K. O.; Stiefel, E. I.; Newton, W. E. *J. Am. Chem. Soc.* **1978**, *100*, 2748.
(35) Wyckoff, R. W. G. *Crystal Structure*, 2nd ed.; Wiley: New York, 1963; Vol. I, p 10.
(36) Troemel, M.; Lupprich, E. *Z. Anorg. Allg. Chem.* **1975**, *414*, 160.

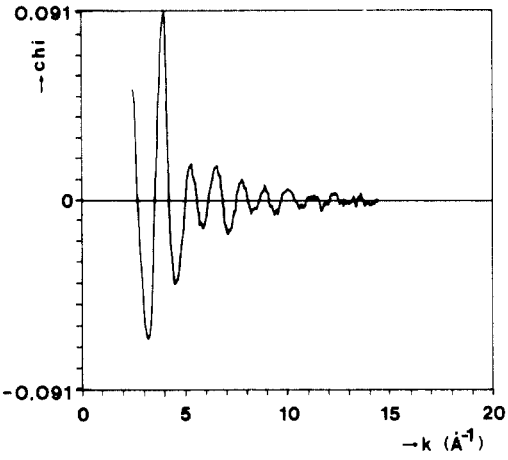

Figure 5. Raw EXAFS of the reaction product of $Os_3(CO)_{12}$ and γ-Al_2O_3.

needed: the calculated Os–Os shell had to be corrected with V_0 = −3.3 eV before the subtraction, and the Os–CO difference spectrum required a correction of V_0 = −4.6 eV. The k^3 weighted Fourier transform of the difference spectrum (experimental results minus calculated Os–Os shell) is presented in Figure 3b. The sidelobe in the Os–O peak in Figure 3a, caused by the Os–Os contribution, has disappeared. The imaginary part of the Os–C contribution peaks positively at the maximum of its Fourier transform, at R = 1.93 Å, which corresponds within the limits of accuracy to the value obtained from crystallographic data (R = 1.95 Å). The Os–O peak has an imaginary part which peaks negatively at the maximum of its magnitude. The peak is located at R = 3.08 Å, which is almost equal to the crystallographic distance of 3.09 Å. This negative imaginary part is caused by multiple scattering (see Discussion). The resulting spectrum in r space (Figure 3b) was back transformed with Δr = 1.20–3.46 Å to give an Os–CO reference. The back transformation spectrum is taken to be reliable as an Os–CO reference only between k =4.2 and 11 Å^{-1}, because of truncation errors in the Fourier transformation procedures.

Triosmium Clusters Chemisorbed on γ-Al_2O_3. The raw EXAFS spectrum of the product formed in the reaction of $Os_3(CO)_{12}$ with the surface of γ-Al_2O_3 is shown in Figure 5. It has been reported[5-7] that the $Os_3(CO)_{12}$ cluster loses two CO ligands when it reacts with oxide supports like Al_2O_3, with the Os_3 skeleton remaining intact.

Comparing the imaginary parts of the Fourier transforms of the parent $Os_3(CO)_{12}$ cluster and the supported cluster shows that strong interferences are present between r = 1.8 and 2.7 Å. This result indicates the presence of an additional scatterer, most probably support oxygen. Between r = 0 and 1.8 Å, the Fourier transform for the supported cluster is very similar to that of the parent $Os_3(CO)_{12}$ cluster. Assuming the commonly accepted structure[5-7] for the supported cluster (shown above), we expect to infer evidence of Os–Os, Os–CO, and Os–$O_{support}$ interactions from the EXAFS data. Of these contributions, the Os–CO contribution is expected to be the greatest and thus the easiest to determine. The loss of two CO ligands per cluster during chemisorption should result in an average EXAFS coordination number N_{Os-CO} = 10/3. When this value for N and the distances R_{Os-C} and R_{Os-O} equal to the values characterizing the unsupported parent cluster (R_{Os-C} = 1.95 Å and R_{Os-O} = 3.09 Å) were used, the EXAFS for an Os–CO shell was calculated. A Debye–Waller factor (relative to the unsupported cluster) of 0.0025 Å^2 was found to give the best agreement in r space (between r = 0 and 1.8 Å) with the experimental results. The experimental results for the supported cluster and the calculated Os–CO shell (both k^1 Fourier transformed, Δk = 4.2–9.0 Å^{-1}, Os–O phase corrected) are shown in Figure 6a.

This calculated Os–CO contribution was subtracted from the experimental results. The difference spectrum should contain at least two contributions, namely the Os–Os and Os–$O_{support}$ shells.

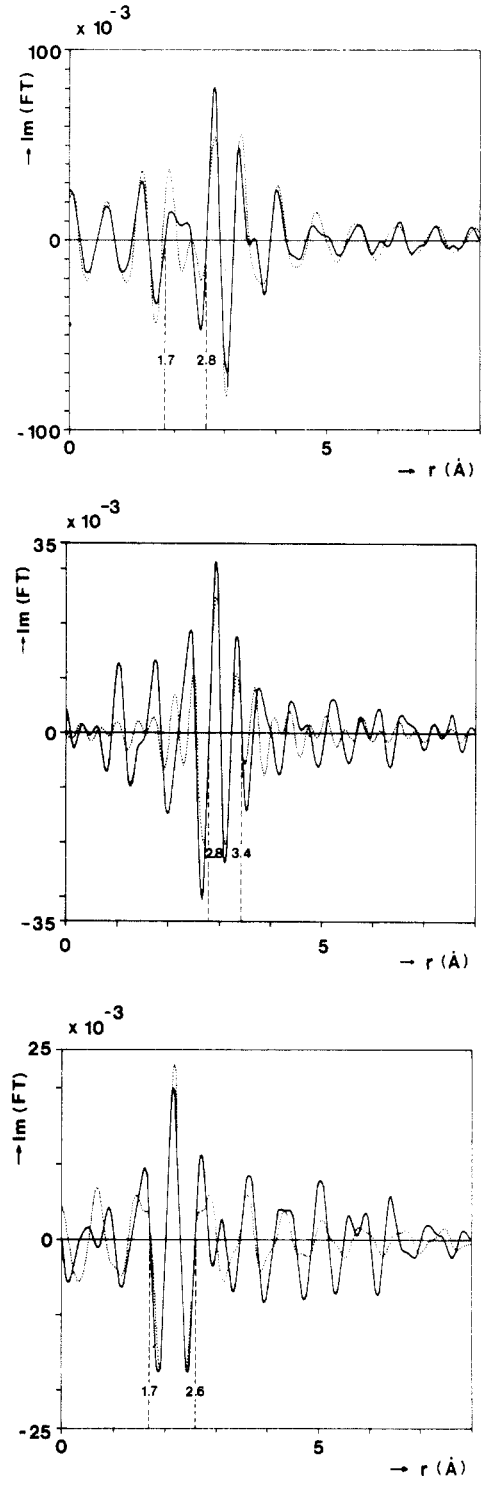

Figure 6. k^1 Fourier transforms (Δk = 4.2–9.0 Å^{-1}) of (a, top) supported cluster formed from $Os_3(CO)_{12}$ and γ-Al_2O_3 (Os–O phase corrected) (solid line) and calculated Os–CO shell (N = 3.35, R_{Os-C} = 1.95 Å, R_{Os-O} = 3.09 Å, $\Delta\sigma^2$ = 0.0025 Å^2 relative to $Os_3(CO)_{12}$, Os–O phase corrected) (dotted line), (b, middle) data for supported cluster minus Os–CO shell (Os–Os phase corrected) (solid line) and calculated Os–Os shell (N = 2, R = 2.88 Å, $\Delta\sigma^2$ = −0.001 Å^2 relative to Pt foil, Os–Os phase corrected) (dotted line), and (c, bottom) data for supported cluster minus Os–CO and Os–Os shells (Os–O phase corrected) (solid line) and calculated Os–$O_{support}$ shell (N = 0.65, R = 2.16 Å, $\Delta\sigma^2$ = −0.004 Å^2 relative to $Na_2Pt(OH)_6$, Os–O phase corrected) (dotted line).

Since it is entirely possible that the Os_3 skeleton is only negligibly affected by the reaction with Al_2O_3, we took the parameters of the Os–Os shell to be those of the unsupported parent cluster (N_{Os-Os} = 2, R_{Os-Os} = 2.88 Å, $\Delta\sigma^2$ = −0.001 Å^2). Fourier transformations of the difference spectrum and the calculated

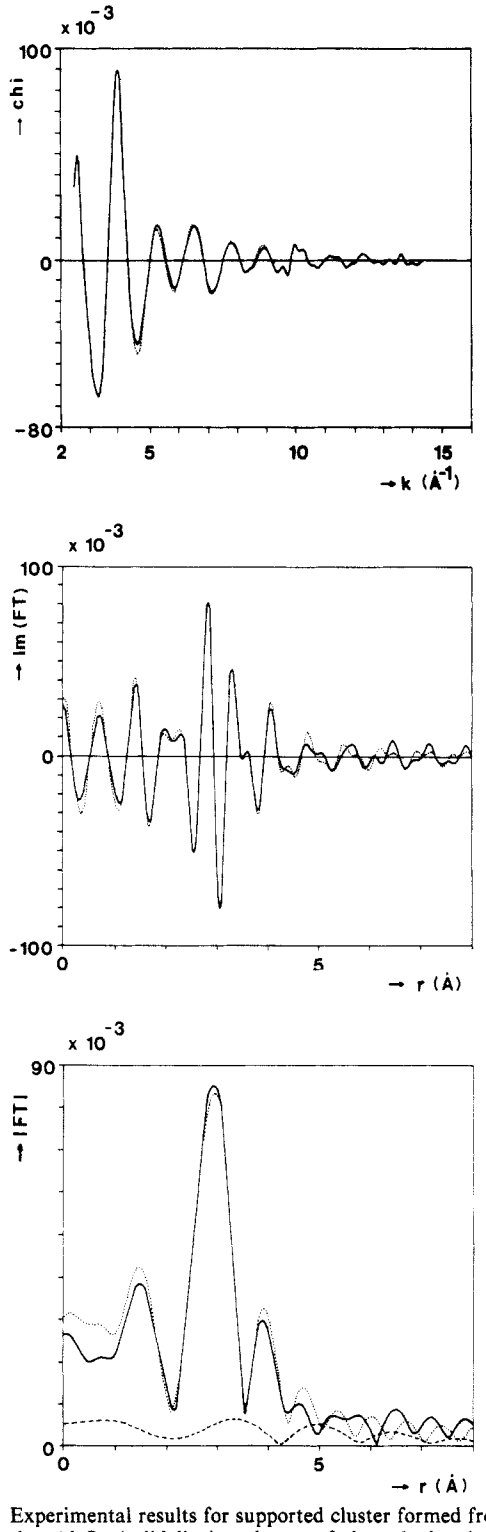

Figure 7. Experimental results for supported cluster formed from $Os_3(CO)_{12}$ and γ-Al_2O_3 (solid line) and sum of the calculated Os–CO, Os–Os, and Os–$O_{support}$ shells (dotted line) (a, top) in k space, (b, middle) in r space (imaginary parts, Δk = 4.2–9.0 Å^{-1}, Os–O phase corrected), and (c, bottom) in r space (magnitude, Δk = 4.2–9.0 Å^{-1}, Os–O phase corrected). Also shown in (c) is the magnitude of the difference between experimental and calculated results (Δk = 4.5–7.5 Å^{-1}, Os–O phase corrected) (dashed line).

Os–Os contribution (k^1, Δk = 4.2–9.0 Å^{-1}, Os–Os phase corrected) showed a good agreement between r = 2.8 and 3.4 Å (Figure 6b). The differences at low r values are caused by Os–$O_{support}$ contributions. Within our limits of precision, we could not find better parameters for the Os–Os shell. The Os–Os coordination distance of 2.88 Å gives the best agreement between the imaginary parts of the Fourier transforms of the calculated and difference spectra. This result stands in contrast to the crystallographic data characterizing $HOs_3(CO)_{10}OSiEt_3$,[11] for which an average Os–Os distance of 2.81 Å was observed.

Table I. Parameters Obtained for the Coordination Shells in $HOs_3(CO)_{10}\{OAl\}$[a]

shell	N	R, Å	$\Delta\sigma^2$, Å^2	ref compd
Os–CO	3.35	1.95 (Os–C) 3.09 (Os–O)	0.0025	$Os_3(CO)_{12}$
Os–Os	2	2.88	−0.001	Pt foil
Os–$O_{support}$	0.65	2.16	−0.004	$Na_2Pt(OH)_6$

[a] Accuracies: N, ±15%; R, ±1%; $\Delta\sigma^2$, ±15%.

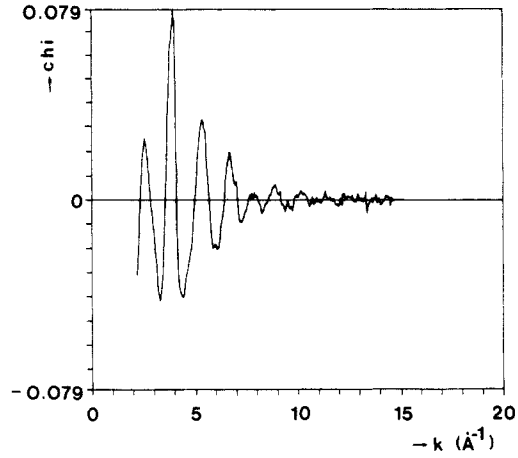

Figure 8. Raw EXAFS of the supported clusters formed from $Os_3(CO)_{12}$ and γ-Al_2O_3 after decomposition in He at 150 °C.

The remainder of the data (experiment minus Os–CO shell minus Os–Os shell) should contain only an Os–$O_{support}$ contribution. One large, symmetrical peak was obtained upon Fourier transformation (k^1, Δk = 4.2–9.0 Å^{-1}, Os–O phase corrected), which is ascribed to an Os–$O_{support}$ interaction (Figure 6c). The Fourier transform of an EXAFS function calculated with N_{Os-O} = 0.65, R_{Os-O} = 2.16 Å, and $\Delta\sigma^2$ = −0.004 Å^2 (relative to $Na_2Pt(OH)_6$) gave the best agreement in r space (between r = 1.7 and 2.6 Å) with the corresponding Fourier transform of the remainder of the data (Figure 6c).

The coordination parameters for all calculated shells are summarized in Table I. To further verify the reliability of the full set of coordination parameters, the calculated EXAFS functions of each individual contribution (Os–CO, Os–Os, and Os–$O_{support}$) were added. It can be seen in Figure 7a that the sum of the calculated contributions agrees very well with the experimental results in k space. Another highly sensitive check of the reliability of the full set of parameters consists of a comparison of the imaginary parts of the corresponding Fourier transforms. Figure 7b shows hardly any differences between the two curves.

Broken-Up Clusters on γ-Al_2O_3. The raw EXAFS data of the decomposed Os cluster are presented in Figure 8. Comparing this spectrum with that of the supported cluster (Figure 5) shows the absence of EXAFS oscillations (due to osmium neighbors) for values of k > 10 Å^{-1}. This result is in agreement with the results of infrared and other experiments, from which it has been concluded that the cluster breakup yields two species, $Os^{II}(CO)_2$ and $Os^{II}(CO)_3$.[5-7] Thus, only Os–CO and Os–$O_{support}$ contributions were expected to be present in the EXAFS of the decomposed cluster. An Os–CO contribution was calculated by using the reference obtained from the $Os_3(CO)_{12}$ data. This calculated contribution was subtracted from the experimental results and the difference spectrum was analyzed for Os–$O_{support}$ contributions. In a recurrent way (described in the Data Analysis section) optimized parameters were found for both coordinations. The best calculation for the Os–CO shell yielded N_{Os-CO} = 2.8, R_{Os-C} = 1.91 Å, R_{Os-O} = 3.05 Å, and $\Delta\sigma^2$ = 0 (relative to $Os_3(CO)_{12}$). The calculated Os–CO shell and the experimental results were Fourier transformed (k^1, Δk = 4.2–8.5 Å^{-1}, Os–O phase corrected; see Figure 9a). The best parameters for the Os–$O_{support}$ shell were found to be N_{Os-O} = 3, R_{Os-O} = 2.17 Å, and $\Delta\sigma^2$ = −0.0025 Å^2

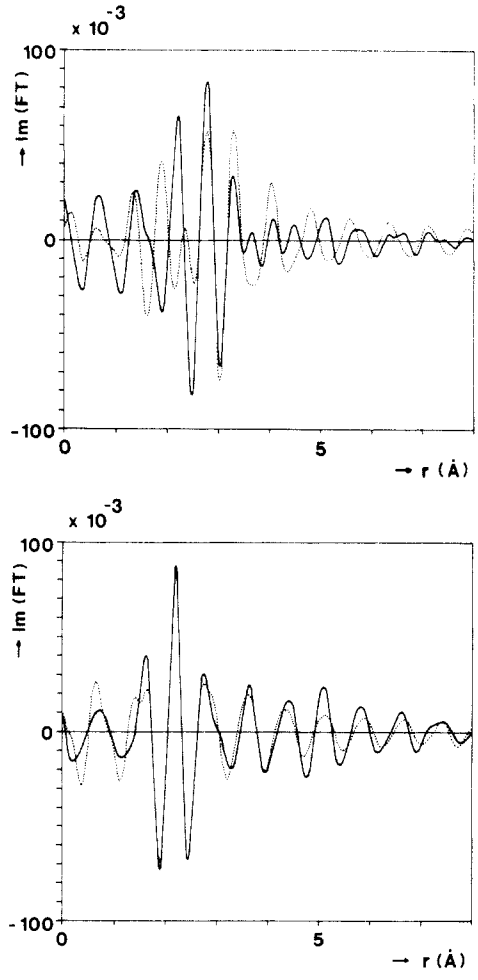

Figure 9. k^1 Fourier transforms (Δk = 4.2–8.5 Å^{-1}; Os–O phase corrected) of (a, top) decomposed cluster data (solid line) and calculated Os–CO shell (N = 2.8, R_{Os-C} = 1.91 Å, R_{Os-O} = 3.05 Å, $\Delta\sigma^2$ = 0 Å^2 relative to $Os_3(CO)_{12}$) (dotted line) and (b, bottom) decomposed cluster data minus Os–CO shell (solid line) and calculated Os–$O_{support}$ shell (N = 3, R = 2.17 Å, $\Delta\sigma^2$ = −0.0025 Å^2 relative to $Na_2Pt(OH)_6$) (dotted line).

(relative to $Na_2Pt(OH)_6$). The calculated Os–$O_{support}$ shell and the difference spectrum were Fourier transformed (k^1, Δk = 4.2–8.5 Å^{-1}, Os–O phase corrected; see Figure 9b). The difference spectrum showed only one peak. Clearly, no detectable Os–Os shell is present.

The sum of the calculated Os–CO and Os–$O_{support}$ shells was Fourier transformed (k^1, Δk = 4.2–8.5 Å^{-1}, Os–O phase corrected) and compared with the experiment (Figure 10). The agreement in k space and in r space is rather good. However, deviations appear at low r values, especially between r = 1.5 and 2 Å.

These deviations are probably caused by changes in the Os—C≡O geometry with respect to the $Os_3(CO)_{12}$ cluster. First, in Os^{II}—C≡O the π-back-bonding effect is inferred to be weaker, resulting in longer Os—C and shorter C≡O distances. Second, we infer that in Os^{II}—C≡O the Os—C—O angle is closer to 180°. This leads to a further enhancement of the Os—(C≡)O shell,[33] while the contribution of the Os—C shell is not affected.

The parameters of the calculated shells are summarized in Table II. The average N_{Os-CO} coordination number of 2.8 supports the results of infrared and other experiments which show that breakup of the supported clusters gives a mixture of $Os^{II}(CO)_2\{OAl\}_3$ and $Os^{II}(CO)_3\{OAl\}_3$ on the Al_2O_3 surface. The analysis shows clear evidence for a coordination of the osmium ion with three oxygen ligands of the γ-Al_2O_3 support.

Discussion

Methods of Data Analysis and Reference Compounds. Interpretation of EXAFS data is sensitive to the assumptions underlying

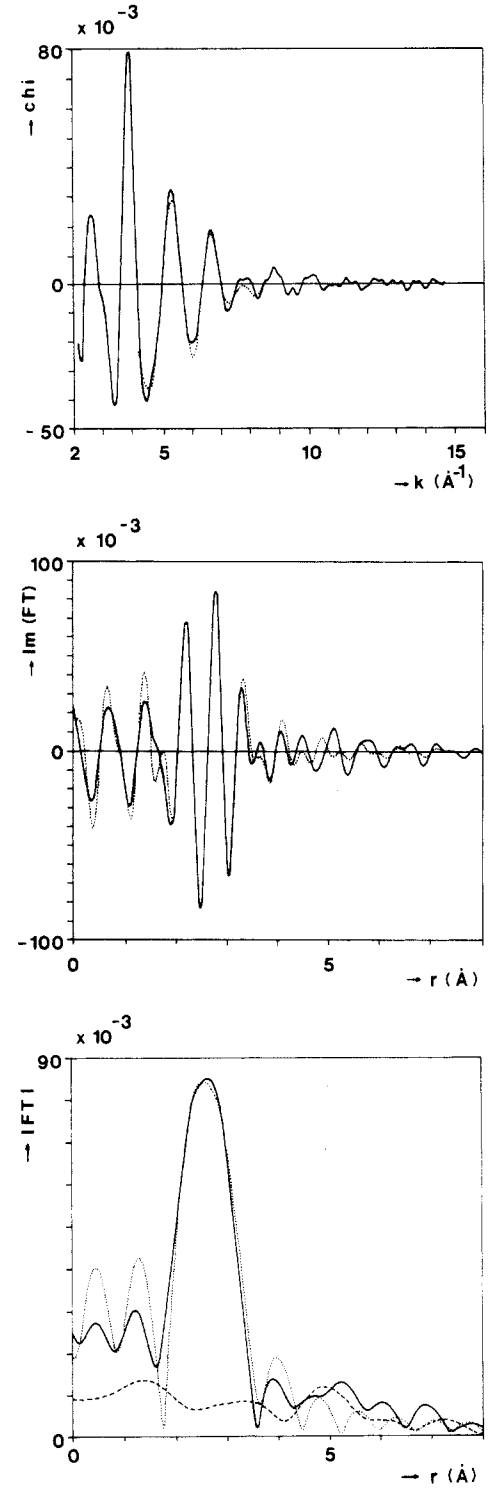

Figure 10. Experimental results characterizing the decomposed clusters on γ-Al_2O_3 (solid line) and the sum of the calculated Os–CO and Os–$O_{support}$ shells (dotted line) (a, top) in k space, (b, middle) in r space (imaginary parts, Δk = 4.2–8.5 Å^{-1}, Os–O phase corrected), and (c, bottom) in r space (magnitude, Δk = 4.2–8.5 Å^{-1}, Os–O phase corrected). Also shown in (c) is the magnitude of the difference between experimental and calculated results (Δk = 4.5–7.5 Å^{-1}, Os–O phase corrected) (dashed line).

Table II. Parameters Obtained for the Coordination Shells in $Os^{II}(CO)_n\{OAl\}_3$ (n = 2 or 3)[a]

shell	N	R, Å	$\Delta\sigma^2$, Å^2	ref compd
Os–CO	2.8	1.91 (Os–C) 3.05 (Os–O)	0	$Os_3(CO)_{12}$
Os–$O_{support}$	3	2.17	−0.0025	$Na_2Pt(OH)_6$

[a] Accuracies: N, ±15%; R, ±1% (Os–C ±5%); $\Delta\sigma^2$, ±15%.

the analysis, and often the assumptions have been less than fully stated in published EXAFS studies; consequently it is difficult to determine the validity of structural models and to compare results presented by different groups. In the next paragraphs the assumptions used in our analysis are evaluated on the basis of the EXAFS technique. Then the results for (1) $Os_3(CO)_{12}$, the reference compound; (2) the supported cluster; and (3) the broken-up cluster on the support are interpreted and compared with data reported in the literature. In the following sections, we evaluate the agreement between the structural models presented in the literature and the EXAFS results, finally drawing some conclusions concerning methodologies for evaluation of EXAFS data and comparing the structures of the supported "molecular" osmium species with those of other supported metals.

A crucial issue in EXAFS spectroscopy is centered on the need for well-characterized reference compounds and the incorporation of EXAFS data characterizing those reference compounds in the interpretation of spectra of less-well-characterized samples. In this work we have collected and used data for a fully characterized reference compound, $Os_3(CO)_{12}$, to account for the Os–CO interactions. We have also used data for platinum metal to analyze the Os–Os interactions and data for the fully characterized compound $Na_2Pt(OH)_6$ to analyze the Os–O interactions.

Calculations of Teo and Lee[26] show that phase and backscattering amplitudes of nearest and next-nearest neighbors in the periodic table are hardly different. The use of phase shifts and backscattering amplitudes obtained from EXAFS data of reference compounds has been shown to be valid in many cases when the chemical state and local structure of the reference and the sample are comparable. Teo and Lee[21] also showed that shifts in the phase function associated with changes in the electronic configuration or oxidation state can be largely compensated by a variation of inner potential. In our analysis we have used the inner potential V_0 as an adjustable parameter. Variations in V_0 arise from uncertainties in the energy calibration and from real edge shifts between the reference material and sample. Since the values of V_0 used in our analyses were always small (<5 eV), we infer that the assumptions concerning the phase transferability are correct.[37]

The data analysis carried out in this work involved the use of phase- and/or amplitude-corrected Fourier transforms, the difference file technique, and fitting in k space. A sensitive criterion was used to estimate the reliability of the parameters, which were determined by the fitting procedures in k space. This consisted of a comparison of the Fourier transform (the imaginary part as well as the magnitude) of the EXAFS function (calculated with these parameters) with the corresponding Fourier transform of the experimental results.

Os–CO Reference. The parent cluster $Os_3(CO)_{12}$ has been used as a reference to characterize the Os—C≡O moiety, since it is expected to be similar in the supported clusters. The Os—C≡O moiety was estimated by subtracting the calculated Os—Os contributions from the experimental EXAFS results obtained for $Os_3(CO)_{12}$. The coordination number (N = 2) and Os–Os distance (2.88 Å, determined by X-ray diffraction for $Os_3(CO)_{12}$) were taken as fixed parameters in the analysis. When a coordination distance of 2.88 Å is used for the calculation of the Os—Os contribution, the (Os—O phase corrected) Fourier transform of the difference file (experimental results minus calculated Os–Os EXAFS, thus representing the Os–CO contribution) has an imaginary part which peaks positively at 1.93 Å (Os–C) and negatively at 3.08 Å (Os–O). These values are equal (within the limits of accuracy) to the corresponding Os–C and Os–O distances found by X-ray diffraction. This comparison demonstrates that the EXAFS results are in agreement with those obtained by X-ray diffraction. No attempt was made to analyze further the data for the $Os_3(CO)_{12}$ cluster itself. The value of the Debye–Waller factor for the Os–Os bond in the cluster determined in the analysis is 0.001 Å^2 smaller than that for the Pt–Pt bond in platinum metal. This result is in agreement with the higher energy of the Os–Os bonds in osmium metal (sublimation energy = 730 kJ/mol) in comparison with that of Pt–Pt bonds in platinum metal (570 kJ/mol).[38]

The occurrence of multiple scattering in the Os–O interaction is shown in the phase-corrected Fourier transform (Figure 3b). The amplitude of the peak at 3 Å is much greater than the value that would be expected on the basis of the simple $1/r^2$ dependence indicated by eq 2. Another indication of multiple scattering is the phase shift of π rad of the Os–O peak, which results in an imaginary part with a negative peak located at the maximum of the magnitude of the Fourier transform. Similar multiple scattering effects have been observed in the Fourier transforms for $(Rh(CO)_2Cl)_2$,[27] $Na_2Fe(CO)_4$,[33] and $Mo(CO)_6$.[34] The EXAFS function obtained by back transformation (not shown) was found to give an excellent representation of the Os—C≡O coordination. Those data were therefore used for the analysis of the EXAFS data characterizing the Os—C≡O moieties in the supported clusters and the broken-up clusters. Since a quantitative theoretical calculation of this multiple scattering process is difficult, even with the best available methods, we expect that experimentally measured values of the phase shift and backscattering amplitude for this moiety will give the most reliable analyses of the EXAFS data.

Assessment of the Structural Models. The starting point in the analysis of the EXAFS data for the supported cluster was the assumption of the $HOs_3(CO)_{10}\{OAl\}$ structure indicated by the stoichiometry of the synthesis from $Os_3(CO)_{12}$ and surface OH groups and the results of infrared, Raman, and electron microscopy experiments mentioned in the Introduction. Therefore, a value of 3.35 (approximately 10/3) was assumed for the number of CO ligands per Os atom, and the number of nearest Os neighbors of each Os atom was taken to be two. The Os–Os distance was taken to be 2.88 Å, which is the distance in crystalline $Os_3(CO)_{12}$. An Os–Os distance of 2.84 Å, as was found in the analysis by Cook et al.[13] of EXAFS data of the triosmium cluster supported on γ-Al_2O_3, leads in our analysis procedure to imaginary parts of the Fourier transforms of the calculated EXAFS contributions which do not match those of the corresponding difference file and experimental results.

The EXAFS results strongly confirm the structural model, being fully consistent with the spectroscopic and stoichiometric data mentioned immediately above. The alumina-supported triosmium cluster is inferred to be one of the best-defined structures on a metal–oxide support. The key to the structural determination is the full spectroscopic characterization, with EXAFS being essential, which is based on comparisons with spectra of analogous molecular structures characterized by X-ray crystallography. We recognize that an improved structural determination of the surface-bound cluster could be obtained from EXAFS with the use of better reference compounds (such as, for example, $HOs_3(CO)_{10}OSiEt_3$[11]). We also emphasize that EXAFS results cannot provide any evidence of the bridging hydride ligand; its existence is based entirely on inference.

The most significant new result characterizing the supported cluster is the determination of the coordination number and average length of the bonds involving the surface oxygen of the support. The average coordination distance was determined clearly by the EXAFS data when the structural assumptions for the Os–CO shell (loss of two CO ligands per cluster upon adsorption) and the Os–Os coordination (N = 2, R = 2.88 Å) were built into the analysis. The average $Os–O_{support}$ coordination number of 0.65 means that two osmium atoms of the Os_3 skeleton are bonded to a surface oxygen of the support. EXAFS cannot distinguish whether one (bridging) oxygen or two oxygen atoms of the support are involved. Chemical arguments support the former.

The absence of any Os–Os oscillations in the experimental EXAFS spectrum and the average Os–CO coordination number of N = 2.8 provide strong confirmation of the structure of the

(37) Lytle, F. W., personal communication. Having both Os metal and Pt metal data available, Dr. Lytle has kindly ascertained that the phase and amplitude of Pt can indeed be used for the analysis of Os data.

(38) Phillips, C. S. G.; Williams, R. J. P. *Inorganic Chemistry*; Clarendon: Oxford, 1966; Part II, p 20.

mononuclear complex formed by breakup of the cluster on the alumina support, $Os^{II}(CO)_n\{OAl\}_3$ ($n = 2$ or 3).[5-7] The structure determination might be improved by use of a reference compound such as the presumably oligomeric $(Os^{II}(CO)_2I_2)$, which has iodide ligands bridging divalent osmium ions. The influence of the M–C–O angle on the experimentally obtained phase and backscattering amplitude needs to be investigated in more detail.

The striking new results characterizing the broken-up cluster are the determination of the number of surface oxygen ions bonded to the osmium and the distance between the Os and these ligands. These results were determined straightforwardly and with a high degree of confidence from the analysis of the EXAFS data. An analogous structure of a metal ion with two CO ligands bonded to three support oxygen ions with a short oxide-type bond length has been reported recently by Van 't Blik et al.[27] This type of surface species was formed during CO chemisorption at room temperature upon very small rhodium metal particles supported on γ-Al_2O_3. The CO chemisorption process induced a disruption of the metal particles leading to a $Rh^I(CO)_2\{OAl\}_3$ complex.

Perspectives on EXAFS of Supported Organometallics and Small Metal Clusters. One of the central research goals in surface catalysis is to relate catalytic properties to structures of well-defined materials. EXAFS can give exact, detailed information about the structures of supported organometallics and small metal aggregates. As shown in this work, EXAFS also can provide precise structural information characterizing the interface (or bonds) between the organometallic species and the support. It is evident that there is fertile ground for further study of organometallics that can serve as structural analogues of metal–support interfaces (as in typical supported metal catalysts). The results can be expected to lead to a better knowledge of metal–support interactions. Decomposition of the supported organometallic cluster into mononuclear complexes followed by a reduction to ultrahighly dispersed metal particles[10,39] provides the possibility to follow with EXAFS the formation of the metal–support interface.

In this work we have determined a distance of 2.17 Å between the osmium ion (formed by decomposition of the triosmium cluster) and the oxygen ion of the support. A recent EXAFS study by Asakura et al.[3] of a decomposed ruthenium cluster on alumina shows a distance of about 2.17 Å between the ruthenium ion and the support oxygen; after reduction in H_2 at 400 °C the formation of small ruthenium entities (consisting of three to four atoms) was observed. Analysis of the EXAFS data by fitting in k space showed the same ionic-type distance between the ruthenium and support oxygen after reduction. A striking feature was the stability of these ruthenium entitites at high temperatures, showing a catalytic behavior different from that of typical ruthenium metal particles ($d > 10$ Å).

(39) Asakura, K.; Yamada, M.; Iwasawa, Y.; Kuroda, H. *Chem. Lett.*, in press.

Covalent-type coordination distances between metal atoms present in the metal–support interface and oxygen ions of the support have been characterized with EXAFS for very small rhodium and platinum metal aggregates (consisting of 5 to 10 atoms) supported on γ-Al_2O_3[1,40,41] and TiO_2.[42,43] The EXAFS signal arising from the metal–support interface for very small metal particles is large enough in comparison to the EXAFS contribution of the metal–metal coordination to allow a reliable determination of the structure of the metal–support interface. For rhodium, a value of about 2.7 Å was found for the coordination distance between a rhodium metal atom ($R \sim 1.3$ Å) and the oxygen ion ($R \sim 1.4$ Å) of the support. This distance is much greater than the distances observed between the atoms in the ruthenium entitites and the support. The rhodium atoms in the small rhodium aggregates were certainly metallic, as determined by XPS,[27] hydrogen chemisorption,[27] and catalytic experiments.[44] On the basis of the results of the catalytic experiments and the EXAFS structural studies reported here and in the literature, we infer that the oxidation state of the ruthenium atoms in the small ruthenium entities[39] is different from zero. More EXAFS investigations are needed to characterize further the bonds present in the metal–support interface.

In summary, the results of this work show the unique value of the well-defined surface-bound organometallics as models of supported metal catalysts. The results provide a firm basis for further EXAFS studies of metal–support interfaces, which will lead to a better understanding of metal–support interactions.

Acknowledgment. We thank R. S. Weber for helpful discussions. The EXAFS experiments were done at SSRL (Stanford University), which is supported by the National Science Foundation (NSF) through the Division of Materials Research and the NIH through the Biotechnology Resource Program in the Division of Research Resources in cooperation with the US Department of Energy. We gratefully acknowledge the assistance of the SSRL staff. The research in Eindhoven was done with financial aid from the Netherlands Organization for the Advancement of Pure Research (ZWO); the research in Delaware was supported by the NSF (Grant CPE-8218311). D.C.K. thanks ZWO for a travel grant (R71-34).

Registry No. $Os_3(CO)_{12}$, 15696-40-9; Os, 7440-04-2.

(40) Koningsberger, D. C.; Van Zon, J. B. A. D.; Van 't Blik, H. F. J.; Visser, G. J.; Prins, R.; Mansour, A. N.; Sayers, D. E.; Short, D. R.; Katzer, J. R. *J. Phys. Chem.* **1985**, *89*, 4075.

(41) Koningsberger, D. C.; Sayers, D. E. *Solid State Ionics* **1985**, *16*, 23.

(42) Koningsberger, D. C.; Martens, J. H. A.; Prins, R.; Short, D. R.; Sayers, D. E. *J. Phys. Chem.*, in press.

(43) Koningsberger, D. C.; Van 't Blik, H. F. J.; Van Zon, J. B. A. D.; Prins, R. *Proceedings of the 8th International Congress on Catalysis*; Verlag Chemie: Weinheim, 1985; Vol. V, p 123.

(44) Van 't Blik, H. F. J. Thesis, Eindhoven University of Technology, 1984.